Pergamon

Bioorganic & Medicinal Chemistry Letters 11 (2001) 1541–1544

BIOORGANIC & MEDICINAL CHEMISTRY LETTERS

Rationale for the Observed COX-2/COX-1 Selectivity of Celecoxib from Monte Carlo Simulations

Melissa L. P. Price and William L. Jorgensen*

Department of Chemistry, Yale University, New Haven, CT 06520, USA

Received 13 July 2000; accepted 1 September 2000

Abstract—Computational studies have yielded an analysis of the contributions to the free energy difference between the binding of celecoxib to COX-1 and to COX-2. The energetic and structural results point to the Ile to Val mutation at residue 523 as the key contributor to COX-2 selectivity; unfavorable steric contact between a sulfonamide oxygen and the δ methyl group of Ile523 destabilizes the complex with COX-1. The His to Arg change at residue 513 is less significant.

Introduction

COX-1 and COX-2 are two isoforms of the enzyme responsible for the cyclooxygenation of arachidonic acid to produce prostaglandins (PGs). The PGs formed by COX-1 protect the gastric mucosa from irritation, while the COX-2-synthesized PGs are involved in the process of inflammation. Traditional nonsteroidal anti-inflammatory drugs (NSAIDs) inhibit the function of both isozymes which results in ulcerogenic side effects.[1] In the last few years, several COX-2-selective drugs have been developed that exhibit reduced incidence of gastrointestinal irritation.[2,3] One such drug, celecoxib (**1**), has been approved for the treatment of arthritis as well as FAP, a genetic disorder leading to colon cancer.

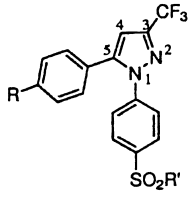

1 R = CH_3; R' = NH_2 (Celecoxib)
2 R = Br; R' = NH_2 (SC-558)
3 R = CH_2CH_3; R' = NH_2
4 R = CH_2OH; R' = NH_2
5 R = OCH_3; R' = NH_2
6 R = F; R' = CH_3 (SC-58125)

While several crystal structures of COX-2 complexed with a ligand in the celecoxib series, SC-558 (**2**), are available in the Protein Data Bank,[4] none have been published for COX-1 complexed with an analogous ligand; the most relevant COX-1 structure is of a complex with flurbiprofen.[5] Comparison of these two structures suggests that the identity of the residue at position 523 affects access to a side-pocket in which the sulfonamide moiety of **1**–**5** binds. In COX-1, isoleucine occupies position 523; valine is the corresponding residue in COX-2. As further support for the role that this residue plays in selectivity, mutagenesis of COX-1[6] and COX-2[7] at this site indicates that the presence of valine instead of isoleucine is sufficient to confer selectivity for a similar ligand, SC-58125 (**6**). In addition to the presence of the smaller valine at position 523, it appears that movement of a tetrapeptide segment in COX-2 enlarges the cavity relative to the analogous space in COX-1.[4]

Recently, we reported calculated binding free energies for a series of celecoxib analogues complexed with both isozymes using the aforementioned crystal structures as starting points.[8] Structural details from these simulations suggested that the steric bulk of Ile523 in COX-1 coupled with the smaller size of the cavity in general, altered the absolute positioning of the phenylsulfonamide ring of the ligand in the complex. Perhaps this strain is at least partially responsible for the reduced affinity of these ligands for COX-1.

In order to characterize the effect of the identity of residue 523 on the binding affinities for the 5-aryl celecoxib derivatives in the absence of the smaller channel size in COX-1, we have calculated the relative free energy of binding for celecoxib (**1**) with COX-2 and its V523I mutant using the Monte Carlo/Free Energy Perturbation method (MC/FEP).

*Corresponding author. Tel.: +1-203-432-6278; fax: +1-203-432-6299; e-mail: bill@adrik.chem.yale.edu

0960-894X/01/$ - see front matter
PII: S0960-894X(00)00522-9

The relative free energies of binding for **1** and **3**–**5** with both the COX-1 and COX-2 wild-type enzymes have also been computed. The energetic and structural details from these MC simulations permit detailed analyses of the origins of COX-2 selectivity.

Computational Methods

Crystal structure coordinates for COX-2 complexed with SC-558 (**2**) and for COX-1 complexed with flurbiprofen were used as initial starting positions (entries 1cx2 and 6cox for COX-2[4,8] and 1prh for COX-1[5]). The initial side-chain conformation of Ile523 in the COX-2 mutant was taken from the COX-1 protein. Residues containing atoms within 15 Å from a ligand atom were explicitly represented in the complex. Ligand **1** was modeled into both wild-type isozymes and the COX-2 mutant, and each complex was conjugate-gradient minimized with a distance-dependent dielectric constant of $4r$.

The MC/FEP calculations were performed in the usual way.[9,10] The backbone conformation was fixed in the position resulting from conjugate gradient minimization. All side-chain bond angles and dihedrals on residues within 10 Å of the ligand center were sampled. Both the ligand and the complex were solvated in a 22 Å cap of TIP4P water,[10] and a 9 Å residue-based cutoff was used. While the entrance to the active site of the enzyme opens into the membrane, neither the crystal structure nor the present calculations include this feature. Each system was equilibrated for 5–10M configurations and the free energies were averaged over an additional 10–20M configurations. The FEP calculations required ca. 10 such runs for the mutation of one ligand to another or of Val to Ile. All parameters were taken from the OPLS-AA force field[12] except that the ligand charges were derived from the CM1A method.[13,14]

Results and Discussion

Biaryl strain

Relative free energies of binding of ligands **1** and **3**–**5** to wild-type COX-1 and COX-2 were computed (Table 1). These values agree with experimental data with an average error of ca. 0.2 kcal/mol. The structural data from the simulations suggest that the 5-aryl ring of the four ligands binds in the same orientation to both isozymes. However, there is an average shift in the position of the phenylsulfonamide ring by ca. 10° in the COX-1 complex compared to the COX-2 complex (Table 2). Geometry optimizations using a dielectric constant of $\varepsilon = 1.5$[15] indicate that both Φ_1 and Φ_2 prefer to be positioned at 315°. A series of minimizations, where Φ_1 is held constant and Φ_2 is varied over 180°, shows that the 10° shift in Φ_2 destabilizes the internal energy of the ligand by over 1 kcal/mol (Fig. 1).

Table 1. Calculated and experimental[a] binding free energies (kcal/mol) of compounds **3**–**5** relative to **1**

	COX-1		COX-2	
Ligand	Calcd[b]	Exptl	Calcd[b]	Exptl
1	0	0	0	0
3	0.38	0.39	1.87	1.82
4	2.12	2.49	4.44	4.59
5	−0.70	−1.04	−0.44	−0.95

[a]Experimental free energies were derived from IC_{50} values[3] via $\Delta G = RT \ln IC_{50}$.
[b]Calculated values have uncertainties of ca. 0.15 kcal/mol.

There is another consideration for the observed ring shift. Since the protein coordinates for COX-1 used in these simulations are from a complex with flurbiprofen, a compound that does not occupy this side pocket, perhaps movement of the protein backbone would permit accommodation of this ligand without perturbing the ligand structure. However, comparison of the COX-2 complexes with flurbiprofen and **2** indicates that no significant conformational changes occur in the side-pocket region when a different ligand is bound.

Residue 523

The free energy changes for the transformation of the COX-2 wild-type protein to its V523I mutant both uncomplexed and bound to **1** were computed. From these two calculations, the relative free energy of binding of the ligand to the two enzymes was determined.[9] The computed $\Delta\Delta G_{binding}$ of 9.7 ± 0.2 kcal/mol is in agreement

Table 2. Average values (in degrees) for dihedral angles governing the positioning of the aryl rings[a]

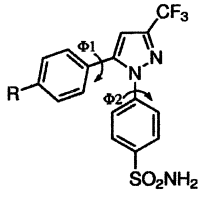

	COX-1		COX-2	
Ligand	Φ_1[b]	Φ_2	Φ_1	Φ_2
1	310.9	333.4	315.2	328.6
3	314.2	334.2	315.5	322.6
4	314.6	338.9	313.0	329.7
5	311.0	336.9	313.4	322.5

[a]Dihedral angles are averaged over 5 million MC configurations.
[b]Φ_1 refers to the C–C–C–C dihedral; Φ_2 corresponds to C–C–N–N.

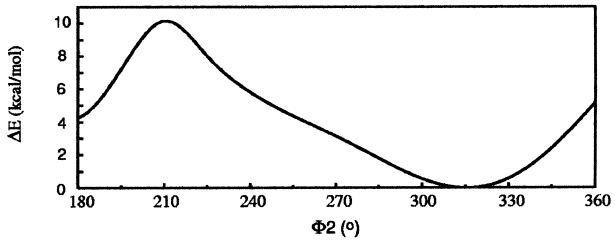

Figure 1. Optimized relative energies as a function of the Φ_2 dihedral angle. Φ_1 was fixed at 315° during these optimizations for **3**.

with the experimental value for the similar ligand **6**[7] as well as with the usual high COX-2/COX-1 selectivity for celecoxib analogues.[3] Possible strain in the COX-1 simulations should be less pronounced in these simulations because of the increased size of the COX-2 binding site relative to COX-1.[4]

A plot of the total $\Delta\Delta G_{binding}$ over the course of the simulation, where $\lambda = 0$ corresponds to the wild-type (Val) COX-2 and $\lambda = 1$ represents the Ile mutant is shown in Figure 2. During the first two-thirds of the perturbation, the total free energy difference closely correlates with the change in intermolecular Lennard–Jones energy ($\Delta\Delta E_{inter}$ L–J).[16] This suggests that the majority of the free energy change arises from a steric penalty between the ligand and the protein that increases as residue 523 is mutated from Val to Ile. At ca. $\lambda = 0.7$, the intramolecular non-bonded energy difference ($\Delta\Delta E_{intra}$) begins to contribute to the $\Delta\Delta G_{binding}$. Analysis of the individual inter-residue energetics indicates that interactions between residue 523 and Gly519 are more unfavorable when residue 523 is Ile compared to Val. The only way that steric contacts for Gly519 can be ameliorated is by adjusting the backbone. Since these simulations do not include backbone sampling, the change in intramolecular energy is likely overestimated and therefore we expect that the true $\Delta\Delta G_{binding}$ may be several kcal/mol less positive.

To identify the source of the $\Delta\Delta E_{inter}$ L–J, we performed single-point energy calculations on complexes of **1** with methyl-capped Ile and Val using geometries from representative configurations of the MC simulations. The interaction energy of the Ile complex is 5.7 kcal/mol less favorable than for the corresponding **1**–Val complex (Fig. 3). Breakdown of the interaction energy by atom pair reveals that two interactions are responsible for 4.5 kcal/mol of the total of 5.7 kcal/mol. One sulfonamide oxygen has a repulsive Lennard–Jones interaction with both the δ-carbon in Ile and with one of its hydrogen atoms. The distances between these atom pairs are 2.76 and 2.40 Å, respectively (Fig. 4a). Optimization of only the intermolecular degrees of freedom increases these interatomic distances. The new O···C distance is 3.57 Å, and the shortest distance from the sulfonamide oxygen to a methyl hydrogen is 2.71 Å (Fig. 4b).

Modeling of this optimized Ile position into the COX-2 mutant protein indicates that the enzyme cannot accommodate the new conformation without rearrangement of the backbone due to unfavorable steric contacts with Gly519 (Fig. 5). This is not surprising considering that steric interactions between these two residues are the largest contributor to the $\Delta\Delta E_{intra}$ in the Val→Ile mutation.

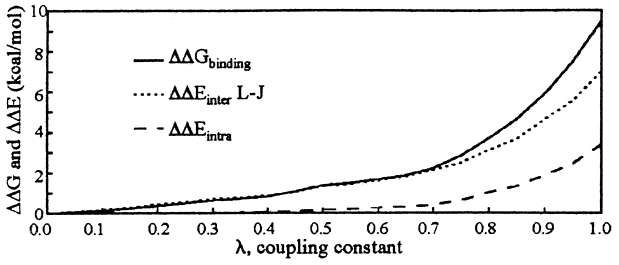

Figure 2. Comparison of the relative bindng free energy of **1** to wild-type and V523I COX-2 with individual energy components.

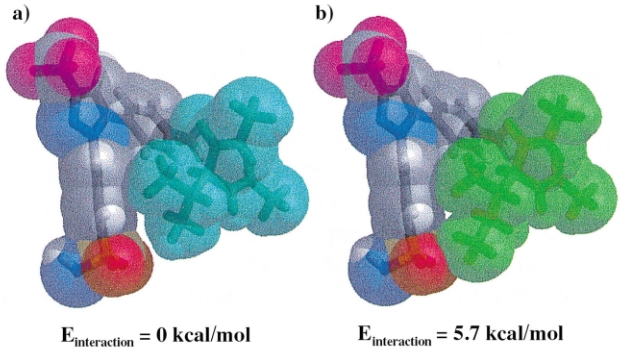

Figure 3. Structure and interaction energy of complexes of **1** with (a) Val and (b) Ile. Geometries are from a single configuration of a Monte Carlo simulation of **1** complexed with the V523I COX-2 mutant at $\lambda = 1.0$. Graphic produced with MidasPlus software.[17]

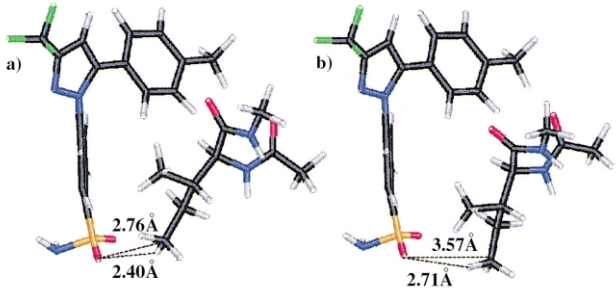

Figure 4. Comparison of the geometry of **1**–Ile complexes from (a) a single representative configuration of an MC simulation and (b) an intermolecular geometry optimization.

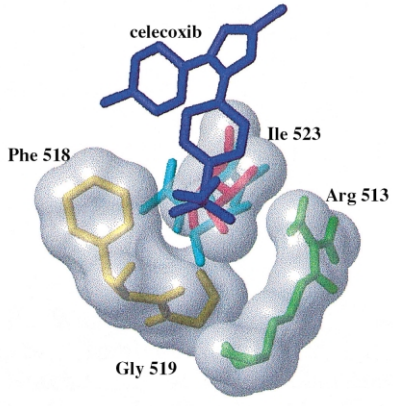

Figure 5. Overlay of selected residues of V523I COX-2 mutant. The red, green, yellow, and dark blue residues as well as the surfaces are from a configuration of an MC simulation. The light blue structure of Ile523 is from the intermolecular geometry optimization. Figure prepared with the program MOLMOL.[18]

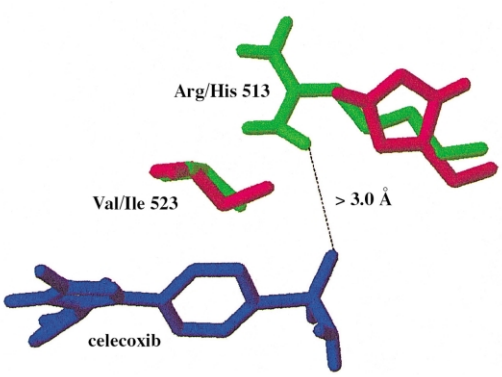

Figure 6. Overlay of wild-type COX-2 (green) and COX-1 (cyan) residues 513 and 523 bound to celecoxib. One representative configuration from an MC simulation is shown. Graphic produced with MOLMOL.[18]

Residue 513

In addition to residue 523, it has been suggested that the residue difference at position 513 between COX-1 (His) and COX-2 (Arg) in the binding site may be partially responsible for the observed selectivity.[4] Because the side chain of His is shorter than that of Arg, it is possible that a sulfonamide oxygen of the ligand can hydrogen bond to the extended Arg in COX-2 but not to His in COX-1 (Fig. 6). Since residue 523 is the only one that differs in our simulations from the wild-type COX-2, the opportunity to maintain this H-bond to Arg513 remains. Structural details show that the bulkier Ile residue does not interfere with the positioning of Arg513. In fact, the arginine does not seem to participate in H-bonding with the ligand even in the wild-type complex. The average distance between the nearest sulfonamide oxygen and H–N on Arg is >3.0 Å. In addition, the O···H–N angle is nonlinear. Therefore, our simulations indicate that residue 513 has little effect on the relative binding affinity for celecoxib. This result is in agreement with the experimental data for **6**.[6]

In summary, though the ligand biaryl strain observed in the COX-1 complexes is not the dominant component of the $\Delta\Delta G_{\text{binding}}$, it is indicative of the steric crunch that results from the 523 Val→Ile substitution. This steric contribution stems from repulsive Lennard–Jones interactions between the δ-methyl group on Ile and a sulfonamide oxygen of the ligand. While it is possible that the additional residue difference between wild-type COX-1 and COX-2 at position 513 also contributes to the selectivity, we see no evidence that the capability of this residue to hydrogen-bond to the ligand plays a significant role.

Acknowledgements

Gratitude is expressed to the National Institutes of Health (GM32136) for support of this work.

References

1. Vane, J. R.; Botting, R. M. *Clinical Significance and Potential of Selective COX-2 Inhibitors*; William Harvey: London, 1998.
2. Prasit, P.; Wang, Z.; Brideau, C.; Chan, C. C.; Charleson, S.; Cromlish, W.; Ethier, D.; Evans, J. F.; Ford-Hutchinson, A. W.; Gauthier, J. Y.; Gordon, R.; Guay, J.; Gresser, M.; Kargman, S.; Kennedy, B.; Leblanc, Y.; Leger, S.; Mancini, J.; O'Neill, G. P.; Ouellet, M.; Percival, M. D.; Perrier, H.; Riendeau, D.; Rodger, I.; Zamboni, R. *Bioorg. Med. Chem. Lett*. **1999**, *9*, 1773.
3. Penning, T. D.; Talley, J. J.; Bertenshaw, S. R.; Carter, J. S.; Collins, P. W.; Docter, S.; Graneto, M. J.; Lee, L. F.; Malecha, J. W.; Miyashiro, J. M.; Rogers, R. S.; Rogier, D. J.; Yu, S. S.; Anderson, G. D.; Burton, E. G.; Cogburn, J. N.; Gregory, S. A.; Koboldt, C. M.; Perkins, W. E.; Seibert, K.; Veenhuizen, A. W.; Zhang, Y. Y.; Isakson, P. C. *J. Med. Chem*. **1997**, *40*, 1347.
4. Kurumbail, R. G.; Stevens, A. M.; Gierse, J. K.; McDonald, J. J.; Stegeman, R. A.; Pak, J. Y.; Gildehaus, D.; Miyashiro, J. M.; Penning, T. D.; Seibert, K.; Isakson, P. C.; Stallings, W. C. *Nature* **1996**, *384*, 644.
5. Picot, D.; Loll, P. J.; Garavito, R. M. *Nature* **1994**, *367*, 243.
6. Wong, E.; Bayly, C.; Waterman, H. L.; Riendeau, D.; Mancini, J. A. *J. Biol. Chem*. **1997**, *272*, 9280.
7. Gierse, J. K.; McDonald, J. J.; Hauser, S. D.; Rangwala, S. H.; Koboldt, C. M.; Seibert, K. *J. Biol. Chem*. **1996**, *271*, 15810.
8. Plount Price, M. L.; Jorgensen, W. L. *J. Am. Chem. Soc*. **2000**, *122*, 9455.
9. Jorgensen, W. L. In *The Encyclopedia of Computational Chemistry*; Schleyer, P. v. R., Allinger, N. L., Clark, T., Gasteiger, J., Kollman, P. A., Schaefer, H. F., Eds.; John Wiley & Sons: Chichester, 1998; pp 1061–1070.
10. Jorgensen, W. L. *MCPRO*, Version 1.6; Yale University: New Haven, 1999.
11. Jorgensen, W. L.; Chandrasekhar, J.; Madura, J. D. *J. Phys. Chem*. **1983**, *79*, 926.
12. Jorgensen, W. L.; Maxwell, D. S.; Tirado-Rives, J. *J. Am. Chem. Soc*. **1996**, *188*, 11225.
13. Storer, J. W.; Giesen, D. J.; Cramer, C. J.; Truhlar, D. G. *J. Comput.-Aided Mol. Des*. **1995**, *9*, 87.
14. Kaminski, G. A.; Jorgensen, W. L. *J. Phys. Chem. B* **1998**, *102*, 1787.
15. Wang, J.; Kollman, P. A.; Kuntz, I. D. *Proteins* **1999**, *36*, 1.
16. In the OPLS-AA force field, the nonbonded energy consists of a Coulombic term to represent electrostatics and a Lennard–Jones 12-6 potential to describe van der Waals interactions. See ref 11.
17. Ferrin, T. E.; Huang, C. C.; Jarvis, L. E.; Langridge, R. *J. Mol. Graphics* **1988**, *6*, 13.
18. Koradi, R.; Billeter, M.; Wüthrich, K. *J. Mol. Graphics* **1996**, *14*, 51.